Supporting Information

Porphyrin-linked Graphdiyne as the substrate for constructing Single-atom Catalyst with transition metal towards Oxygen reduction reaction and Oxygen evolution reaction

Jiejie Ping,‡[a] Mei Wu,‡[b] Manyu Liu,[a] Yan Jiang,[a] Wenhui Shang,[a] Menggai Jiao,*[c] Jiahao Ruan,[b] Nan Wang,*[a] Zhiyu Jia*[a]

a. MOE Key Laboratroy of Cluster Science, Beijing Key Laboratory of Photoelectronic/Electrophotonic Conversion Materials, School of Chemistry and Chemical Engineering, Beijing Institute of Technology, Beijing 100081, P. R. China.

b. School of Engineering, China University of Petroleum-Beijing at Karamay, Xinjiang, 834000, P. R. China.

c. Interdisciplinary Research Center for Sustainable Energy Science and Engineering (IRC4SE[2]), School of Chemical Engineering, Zhengzhou University, Zhengzhou 450001, P. R. China

E-mail address: jzy@bit.edu.cn (Z. Jia); nanwang@bit.edu.cn (N. Wang); mgjiao@zzu.edu.cn (M. Jiao).

1. Synthesis of TM@TEPP
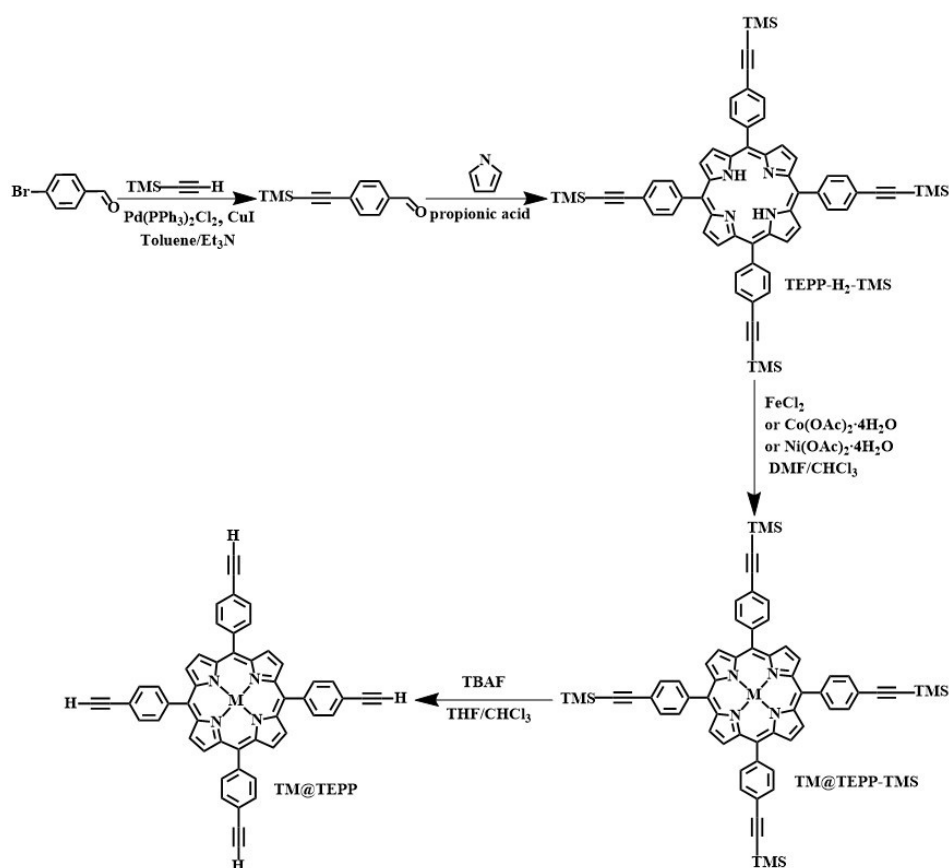
Scheme 1. Synthetic route for TM@TEPP (TM = Fe, Co, Ni)

The detailed synthetic procedure for TM@TEPP (TM = Fe, Co, Ni) is depicted in Scheme 1, and the corresponding experimental process are outlined below:

Synthesis of 4-(trimethylsilylethynyl)benzaldehyde:

A 250 mL three-necked flask was charged with 50 mL of toluene and 50 mL of triethylamine, after which nitrogen gas was purged through the solution. To this flask, 4-bromobenzaldehyde (25 mmol, 4.63 g) was added, followed by the introduction of Pd(PPh₃)₂Cl₂ (0.5 mol %, 0.35 g) and CuI (1 mol %, 0.191 g). After the reaction, the mixture was transferred to a flask, the excess solvent was removed on a rotary evaporator, and the remaining part was transferred to a separatory funnel for extraction, and saturated saline (20 mL) and dichloromethane (20 mL × 3) were added. The organic layer was dried and concentrated again using a rotary evaporator. The concentrated organic layer was purified by silica gel column chromatography using petroleum ether and ethyl acetate 4:1 as the eluent to obtain the white powder 4.46 g in 88% yield.

Synthesis of 5,10,15,20-tetrakis(4-trimethylsilyl-ethynylphenyl)porphyrin (TEPP-H$_2$-TMS): Propionic acid (40 mL) was placed in a 100 mL three-neck flask, 4-(trimethylsilylethynyl)benzaldehyde (1.01 g, 5 mmol) was added and stirred at 100 ºC for 1 h. Then pyrrole (0.35 mL, 5 mmol) was added dropwise to the three-necked flask and refluxed at 100 ºC for 3 h. During the reaction, aluminum foil was used to shield the light. After cooled to room temperature, the mixture was extracted and washed 3 times with methanol. Then obtained a purple solid 0.27 g in 22% yield.

Synthesis of 5, 10, 15, 20-tetrakis(4-trimethylsilyl-ethynylphenyl) metalloporphyrin (TM@TEPP-TMS): 25 mL of DMF and 10 mL of trichloromethane were added to a 100 mL three-necked flask, and TEPP-H$_2$-TMS (250 mg, 0.25 mmol) and FeCl$_2$ (0.25 g, 2 mmol) were weighed into the three-necked bottles and heated at 120 ºC for 12 hours. After cooling to room temperature, trichloromethane was removed under reduced pressure using a rotary evaporator, and then deionized water was added to a flask and the solid was filtered, washed three times with deionized water and dried to obtain purple-black crystals of Fe@TEPP-TMS. The FeCl$_2$ (0.25 g, 2 mmol) was replaced by Co(OAc)$_2$·4H$_2$O (0.62 g, 2.5 mmol) for the preparation of Fe@TEPP-TMS. Ni@TEPP-TMS was prepared by replacing FeCl$_2$ (0.25 g, 2 mmol) with Ni(OAc)$_2$·4H$_2$O (0.62 g, 2.5 mmol).

Synthesis of 5, 10, 15, 20-tetra(4-ethynylphenyl)metalloporphyrin (TM@TEPP): The metalloporphyrin TM@TEPP-TMS (0.26 g) was dissolved in 35 mL of THF. Add liquid nitrogen to ethyl acetate to bring the temperature to -78 ºC. Add 2 mL of TBAF to the solution and stir continuously. Allow the temperature to rise slowly from -78ºC to room temperature and maintain overnight. After completion of the reaction, the reaction was concentrated by spin evaporation and the concentrate was added to a separatory funnel and extracted with 150 mL of water and 3 × 150 mL of trichloromethane. The organic phase was dried with anhydrous Na$_2$SO$_4$ and the resulting light purple solid could be used directly in the next reaction step.

Electrode preparation

Oxygen reduction reaction (ORR): First, two copper sheets (2 × 2 cm^2) were sonicated with acetone, 1 M HCl, deionized water, and ethanol for 5 min, respectively. The dried copper sheets were placed into a 250 mL three-necked flask, to which 40 mL of pyridine was added and nitrogen gas was passed. Then dissolve 200 mg of TM@TEPP in pyridine (25 mL), drop this solution into the three-necked flask, and reflux at 120 ℃ for 3 days. After the reaction, the copper sheets were washed with anhydrous ethanol, dried in a vacuum oven at 60 ℃. The polymerized TM@TEPPD powder was washed with deionized water and anhydrous ethanol, respectively. The dried powder was heated in tube furnace under argon atmosphere at a heating rate of 5 °C min^{-1} up to the present temperature for 4 h. The heat-treated samples were then sonicated with 0.5 M HNO$_3$ for 30 min and then leached in 1 M HCl solution for 12 hours. The acid-washed samples were washed with deionized water and anhydrous ethanol, respectively. Eventually, the samples were dried to obtain a black powdered product.

Oxygen evolution reaction (OER): First, a carbon cloth (4 × 4 cm^2) was sonicated with acetone, 1 M HCl, deionized water, and ethanol for 5 min, then dried in a vacuum oven at 60 ℃. Second, dried carbon cloth and copper sheet (2 × 2 cm^2, which have been pre-treated by the same process of ORR) were put into a 250 mL three-necked flask, to which 40 mL of pyridine was added and nitrogen gas was introduced. Then dissolve 33 mg of TM@TEPP with 25 mL of pyridine, drop this solution into the three-necked flask, and reflux at 120 ℃ for 2.5 days. After the reaction, the carbon cloth was washed with anhydrous ethanol and dried in a vacuum oven at 60 ℃.

Electrochemical measurement

ORR testing procedure:

The ORR activity of the prepared catalysts was tested by cyclic voltammetry (CV) and rotating ring-disk electrode (RRDE) on an electrochemical workstation (CHI. 760E, Shanghai CH. Instruments, China) with a typical three-electrode system. The glassy carbon RRDE (d = 4 mm) with the as-prepared samples, saturated calomel electrode (SCE), and Pt wire were used as the working electrode, reference electrode, and counter electrode, respectively. ORR experiments were carried out in 0.1 M KOH. The potential was scanned between 1.1-0.1 (V vs. RHE) at a scan rate of 10 mV s^{-1} at room temperature after the introduction of O_2 or N_2 gas for 30 min. All working electrodes were prepared as follows: 5 mg of catalyst, 30 μL of Nafion solution (5 wt%) were dispersed in the mixture of anhydrous ethanol (320 μL) and deionized water (650 μL), and then the above mixture was sonicated for 3 h to form a homogeneous ink. Then 10 μL of ink was loaded onto a polished glassy carbon rotating disc electrode with 0.1256 cm^2 and the electrode was dried at room temperature. The background current was measured under nitrogen saturation before the measurement. Then O_2 was passed to saturate the solution. The catalyst loading on the working electrode was 0.4 mg cm^{-2} in 0.1 M KOH. All potentials were calibrated as reversible hydrogen electrodes (E_{RHE} = $E_{measured}$ + E_{SCE} + 0.059 × pH)

OER testing procedure:

Electrochemical measurements were performed on an electrochemical workstation (CHI. 760E, Shanghai CH. Instruments, China) with a typical three-electrode system. The as-prepared samples, saturated calomel electrode (SCE), and graphite plate were used as the working electrode, reference electrode, and counter electrode, respectively. The measurement area is 1 × 1 cm^2. Polarization curves were collected in 1.0 M KOH at 5 mV s^{-1}. The electrolyte was degassed by Ar before starting the experiment. Cyclic voltammogram measurements were conducted within -1~1 V at 100 mV s^{-1}. All potentials were converted to the reversible hydrogen electrode (RHE, E_{RHE} = $E_{measured}$ + E_{SCE} + 0.059 × pH). LSV curves were performed at the scan rate of 5 mV s^{-1}. Tafel slopes were calculated according to the Tafel equation: η = blog j + a. The EIS measurements were investigated at frequencies from 100 kHz to 0.1 Hz.
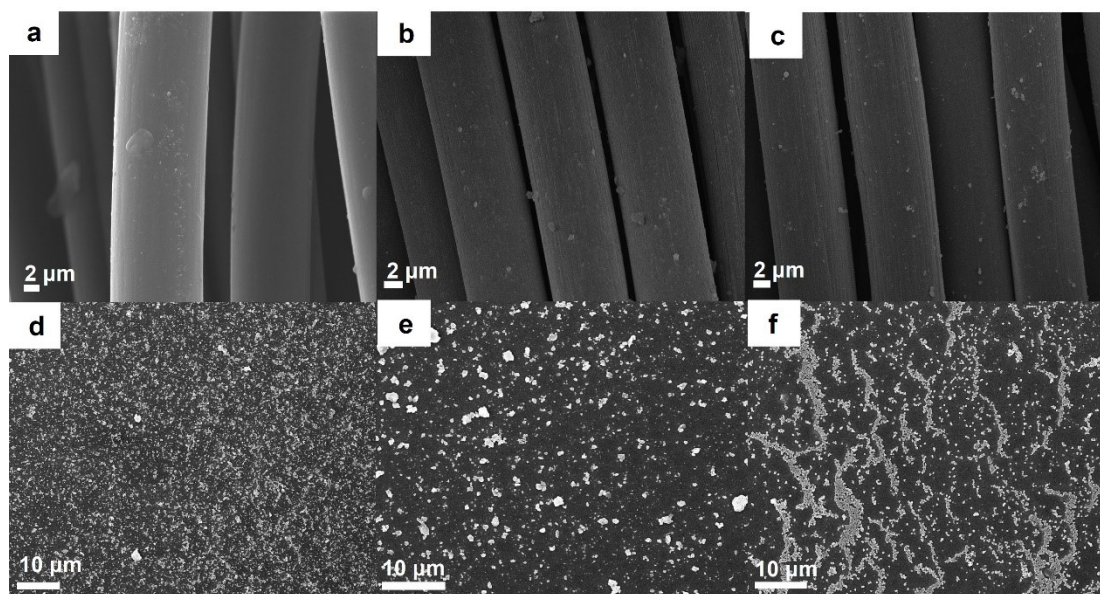
Figure S1. SEM images of Fe@ PGDY (a), Co@ PGDY (b) and Ni@ PGDY (c) on carbon cloth; SEM images of the powder of Fe@PGDY (d), Co@ PGDY (e) and Ni@ PGDY (f).
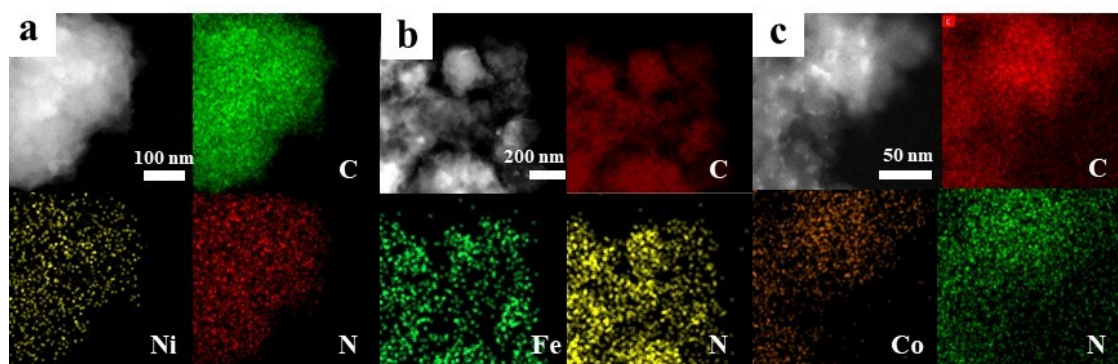

Figure S2. Scanning TEM image and the corresponding element mapping about the TM, C and N of Ni@ PGDY (a); Fe@ PGDY (b) and Co@ PGDY (c).
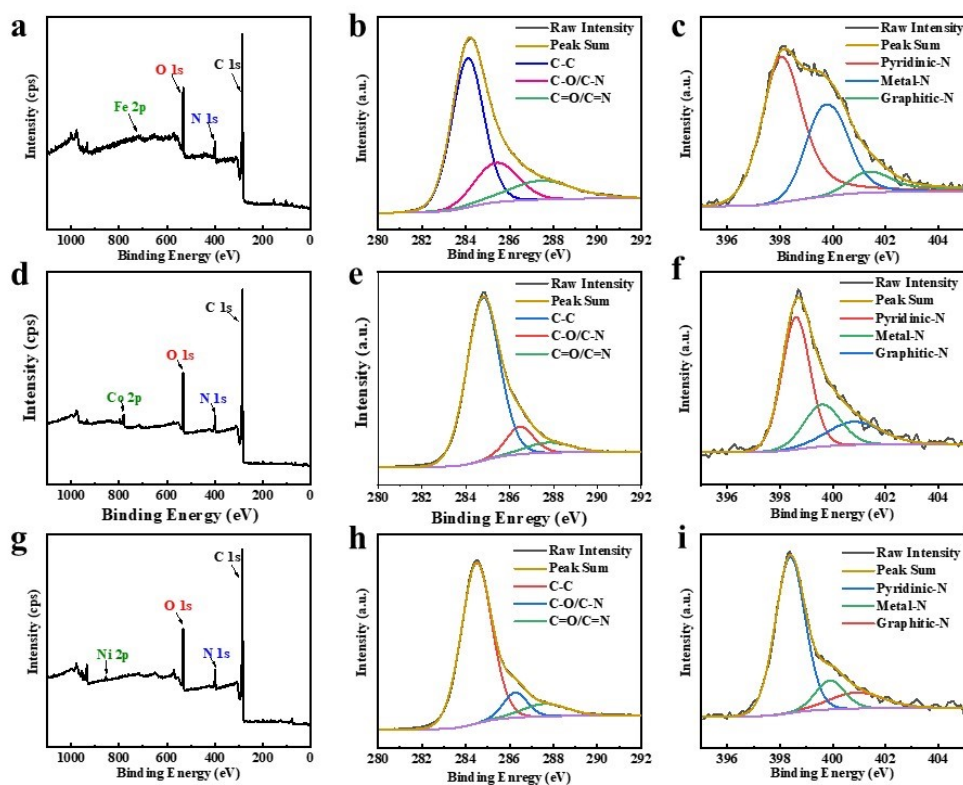
Figure S3. XPS spectrum of Fe@ PGDY (a), high-resolution XPS spectrums of C 1s (b) and N 1s (c); XPS survey spectrum of Co@PGDY (d), high-resolution XPS spectrums of C 1s (e) and N 1s (f); XPS survey spectrum of Ni@PGDY (g), high-resolution XPS spectrums of C 1s (h) and N 1s (i).
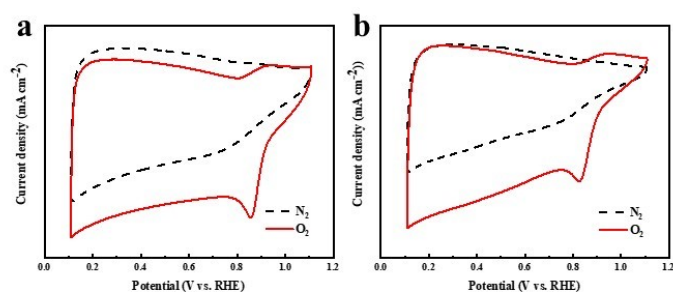

Figure S4. (a) CV curves of Co@PGDY under N_2-saturated and O_2-saturated 0.1 M KOH solution; (b) CV curves of Ni@PGDY under N_2-saturated and O_2-saturated 0.1 M KOH solution.
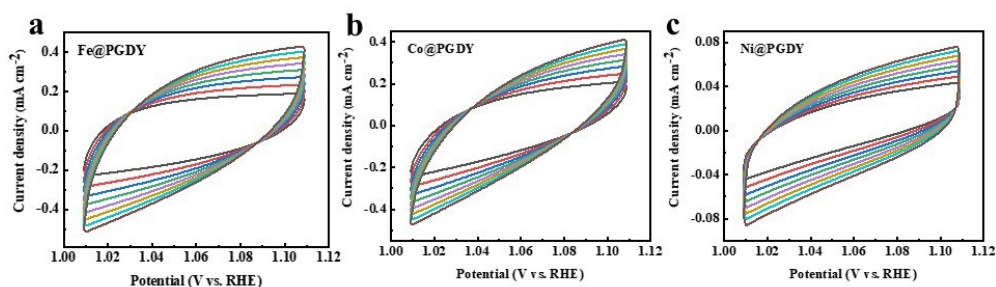
Figure S5. CV curves of Fe@PGDY (a), Co@PGDY (b) and Ni@PGDY (c) in 0.1 M KOH solution at scan rates of 15, 20, 25, 35, 30, 35, 40, 45, and 50 mV s^{-1}, respectively.
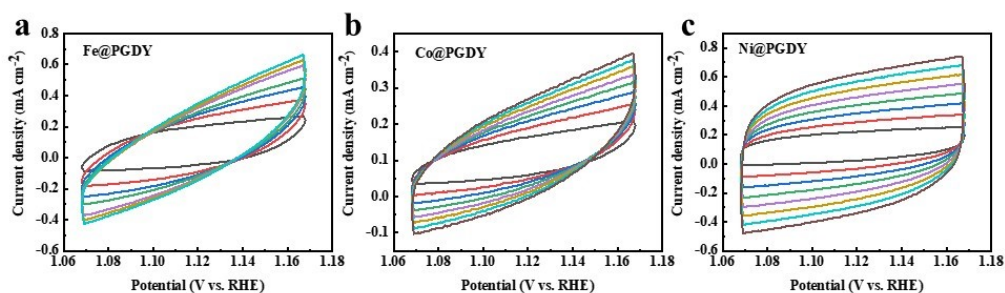

Figure S6. CV curves of Fe@PGDY (a), Co@PGDY (b) and Ni@PGDY (c) in 1 M KOH solution at scan rates of 20, 40, 60, 80, 100, 120, 140 and 160 mV s^{-1}, respectively.
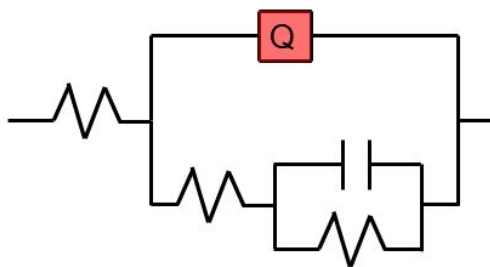

Figure S7. The circuit equivalent model used for the data fitting of TM@PGDY.
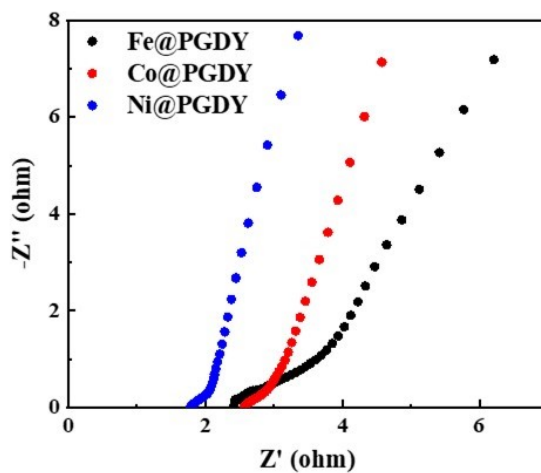

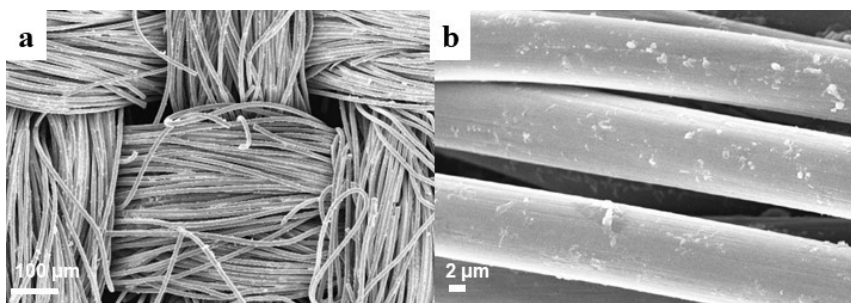**Figure S8.** EIS Nyquist of Fe@PGDY, Co@PGDY and Ni@PGDY

Figure S9. The SEM image of the Ni@PGDY electrode after OER, (a) the overview SEM image; (b) high-magnification SEM image.

Table S1. Fitting parameters of Fe@PGDY standard (N: coordination number; R: distance; σ^2: mean-square disorder; E_0: energy shift). The single-digit numbers in parentheses are the last digit errors.

Sample	Path	N	R (Å)	σ^2 ($\times 10^{-3}$ Å^2)	ΔE_0 (eV)	R-factor
Fe foil	Fe-Fe	12	☐	☐	☐	☐
Fe$_2$O$_3$	Fe-O	6				
Fe-N-C	Fe-N	3.8	2.05	3.6	9.87	0.034

Table S2. Fitting parameters of the Ni@ PGDY (NiN$_3$) standard (N: coordination number; R: distance; σ^2: mean-square disorder; E_0: energy shift). The single-digit numbers in parentheses are the last digit errors.

Sample	Path	N	R (Å)	$\sigma2$ ($\times 10^{-3}$ Å^2)	ΔE_0 (eV)	R-factor
Ni foil	Ni-Ni	12	☐	☐	☐	☐
NiO	Ni-O	6				
Ni-N-C	Ni-N	3	1.9	4.4	-0.68	0.031

Table S3. Literature survey on overpotential of other catalysts for ORR in 0.1 M KOH.

Entry	Electrocatalysts	$E_{1/2}$ (V)	References
1	Fe@PGDY	0.87	*This work*
2	CoTAPP-PATA-COF	0.80	Ref. 1
3	Co TPP/CNT	0.81	Ref. 2
4	PCN-226-Co/C	0.75	Ref. 3
5	F_5NCo	0.85	Ref. 4
6	cov FeTPP-CNT	0.64	Ref. 5
7	TTBPP-Co	0.76	Ref. 6
8	BA-TPACoP/CNT	0.85	Ref. 7
9	Bz-2TCoP/C	0.77	Ref. 8
10	Co-2	0.86	Ref. 9
11	TAPPCo–QA	0.78	Ref. 10

Table S4. Literature survey on $E_{1/2}$ of other catalysts for OER in 1 M KOH.

Entry	Electrocatalysts	η at 100 mA cm^{-2} (mV)	References
1	Ni@ PGDY	687	*This work*
2	G$_{ZnP-PhCN-1}$	>687	Ref. 11
3	1/MWCNT/Py–Py	>687	Ref. 12
4	NiCo$_2$S$_4$/CNNs$_{-1}$	>687	Ref. 13
5	Fe$_2$P/Fe$_4$N@C-800	>687	Ref. 14
6	NiTAPP-NA	>687	Ref. 15
7	TA-PPy/CP	>687	Ref. 16
8	CPF2	>687	Ref. 17

References：

1. M. Liu, S. Liu, C.-X. Cui, Q. Miao, Y. He, X. Li, Q. Xu and G. Zeng, *Angew. Chem., Int. Ed.*, 2022, **61**, e202213522.

2. H. Qin, Y. Wang, B. Wang, X. Duan, H. Lei, X. Zhang, H. Zheng, W. Zhang and R. Cao, *J. Energy Chem.*, 2021, **53**, 77.

3. M. O. Cichocka, Z. Liang, D. Feng, S. Back, S. Siahrostami, X. Wang, L. Samperisi, Y. Sun, H. Xu, N. Hedin, H. Zheng, X. Zou, H.-C. Zhou and Z. Huang, *J. Am. Chem. Soc.*, 2020, **142**, 15386.

4. Y. Dong, X. Lv, Y. Sun, Q. Zhao, H. Lei, F. Wu, T. Zhang, Z. Xue, R. Cao, F. Qiu and S. Xue, *Inorg. Chem.*, 2024, **63**, 4797.

5. Q. Li, Y. Xu, A. Pedersen, M. Wang, M. Zhang, J. Feng, H. Luo, M. M. Titirici and C. R. Jones, *Adv. Funct. Mater.*, 2023, 2311086.

6. Y.-F. Yao, W.-Y. Xie, S.-J. Huang, J.-S. Ye, H.-Y. Liu and X.-Y. Xiao, *J. Electroanal. Chem.*, 2024, **952**, 117987.

7. Y. Wei, L. Zhao, Y. Liang, M. Yuan, Q. Wu, Z. Xue, X. Qiu and J. Zhang, *Chem. Eng. J.*, 2023, **476**, 146575.

8. Y. Wei, Y. Liang, Q. Wu, Z. Xue, L. Feng, J. Zhang and L. Zhao, *Dalton Trans.*, 2023, **52**, 14573.

9. S. Xue, W. Ryan Osterloh, X. Lv, N. Liu, Y. Gao, H. Lei, Y. Fang, Z. Sun, P. Mei, D. Kuzuhara, N. Aratani, H. Yamada, R. Cao, K. M. Kadish and F. Qiu, *Angew. Chem., Int. Ed.*, 2023, **62**, e202218567.

10. R. Ren, L. Yang, Z. Lin, X. Li, S. Zhang, T. Zheng, D. Wu, J. Wang, Z. Wei, W. Ding, N. Huang, M. Gu and Q. He, *J. Mater. Chem. A*, 2022, **10**, 22781.

11. B.-O. Taranu and E. Fagadar-Cosma, *Nanomater.*, 2022, **12**, 3788.

12. I. K. Attatsi, W. Zhu and X. Liang, *New J. Chem.*, 2020, **44**, 4340.

13. J.-Z. He, W.-J. Niu, Y.-P. Wang, Q.-Q. Sun, M.-J. Liu, K. Wang, W.-W. Liu, M.-C. Liu, F.-C. Yu and Y.-L. Chueh, *Electrochimi. Acta*, 2020, **362**, 136968.

14. X. Fan, F. Kong, A. Kong, A. Chen, Z. Zhou and Y. Shan, *ACS Appl. Mater. Interfaces*, 2017, **9**, 32840.

15. G. Cai, L. Zeng, L. He, S. Sun, Y. Tong and J. Zhang, *Chem. Asian J.*, 2020, **15**, 1963.

16. L. Hu, X. Tan, J. Chen, L. Xu, R. Luo, X. Wu, X. Wen, S. Zhang and Z. Fei, *Int. J. Hydrogen Energy*, 2024, **58**, 621.

17. N. Gupta, S. Kanungo, R. P. Behere, P. Singh, S. Kanungo, M. Dixit, C. Chakraborty and B. K. Kuila, *ACS Appl. Mater. Interfaces*, 2023, **15**, 29042.